Cause or consequence? Exploring the role of phenotypic plasticity and genetic polymorphism in the emergence of phenotypic spatial patterns of the European eel

M. Mateo, Patrick Lambert, S. Tétard, M. Castonguay, B. Ernande, Hilaire Drouineau

HAL Id: hal-01548904

https://hal.science/hal-01548904

Submitted on 28 Jun 2017

1   Cause or consequence? Exploring the role of phenotypic plasticity and genetic polymorphism in the

2   emergence of phenotypic spatial patterns of the European eel

3

4   Authors:

5   • Maria MATEO (corresponding author)

6   ○ Affiliations: Irstea, UR EABX Ecosystèmes aquatiques et changements globaux, HYNES

7   Irstea – EDF R&D

8   ○ Address: 50 avenue du Verdun, 33 612 Cestas, France

9   ○ Tel: +33 (0)5 57 89 09 98

10   ○ Email: maria.mateo@irstea.fr

11   • Patrick LAMBERT

12   ○ Affiliations: Irstea, UR EABX Ecosystèmes aquatiques et changements globaux, HYNES

13   Irstea – EDF R&D

14   ○ Address: 50 avenue du Verdun, 33 612 Cestas, France

15   ○ Email: patrick.lambert@irstea.fr

16   • Stéphane TETARD

17   ○ Affiliations: EDF R&D, HYNES Irstea – EDF R&D, Laboratoire National d'Hydraulique et

18   Environnement

19   ○ Address: 6 quai Watier, 78 401 Chatou, France

20   ○ Email: stephane.tetard@edf.fr

21   • Martin CASTONGUAY

22   ○ Affiliations: Ministère des Pêches et des Océans, Institut Maurice-Lamontagne

23   ○ Address: C.P. 1000, 850, route de la Mer, Mont-Joli, QC G5H 3Z4, Canada

24   ○ Email: Martin.Castonguay@dfo-mpo.gc.ca

25   • Bruno ERNANDE

26   ○ Affiliations: IFREMER, Laboratoire Ressources Halieutiques de Boulogne

27   o   Address: 150 Quai Gambetta, BP 699, 62 321 Boulogne-sur-Mer, France

28   o   Email: bruno.ernande@ifremer.fr

29   •   Hilaire DROUINEAU

30   o   Affiliations: Irstea, UR EABX Ecosystèmes aquatiques et changements globaux, HYNES

31   Irstea – EDF R&D

32   o   Address: 50 avenue du Verdun, 33 612 Cestas, France

33   o   Email: hilaire.drouineau@irstea.fr

1 Abstract

35   The European eel (*Anguilla anguilla*), and generally, temperate eels, are relevant species for

36   studying adaptive mechanisms to environmental variability because of their large distribution areas

37   and their limited capacity of local adaptation. In this context, GenEveel, an individual-based

38   optimization model, was developed to explore the role of adaptive phenotypic plasticity and genetic-

39   dependent habitat selection, in the emergence of observed spatial life-history traits patterns for eels.

40   Results suggest that an interaction of genetically and environmentally controlled growth may be the

41   basis for genotype-dependent habitat selection, whereas plasticity plays a role in changes in life-

42   history traits and demographic attributes. Therefore, this suggests that those mechanisms are

43   responses to address environmental heterogeneity. Moreover, this brings new elements to explain

44   the different life strategies of males and females. A sensitivity analysis showed that the parameters

45   associated with the optimization of fitness and growth genotype were crucial in reproducing the

46   spatial life-history patterns. Finally, it raises the question of the impact of anthropogenic pressures

47   that can cause direct mortalities but also modify demographic traits, and act as a selection pressure.

48

49   Keywords: phenotypic plasticity, *Anguilla anguilla*, genetic polymorphism, life history theory,

50   modeling

2 Introduction

51

52   Life-history theory posits that the schedule and duration of life-history traits are the result of

53 natural selection to optimize individual fitness (Clark 1993; Giske et al. 1998). Optimal solutions

54 greatly depend on environmental conditions, and consequently, living organisms have developed

55 different adaptive mechanisms to address environmental variability. Among them, local adaptation

56 theory posits that natural selection favors the most well adapted genotypes in each type of

57 environment. In a context of limited genetic exchange between environments, this may lead to

58 isolation and speciation (Williams 1996; Kawecki and Ebert 2004). Phenotypic plasticity might also be

59 an adaptive response to an heterogeneous environment (Levins 1963; Gotthard and Nylin 1995;

60 Pigliucci 2005). Phenotypic plasticity refers to the possibility of a genotype to produce different

61 phenotypes depending on environmental conditions. In some cases, increases in fitness occur

62 because of plastic phenotypes compared to non-plastic ones, and that consequently, phenotypic

63 plasticity may be selected by natural selection (Schlichting 1986; Sultan 1987; Travis 1994).

64   Adaptation to environment heterogeneity is a key issue for temperate anguilids, *Anguilla*

65 *anguilla*, *A. japonica*, *A. rostrata,* three catadromous species that display remarkable similarities in

66 their life-history traits (Daverat et al. 2006; Edeline 2007). The European eel (*A. anguilla*) is widely

67 distributed from Norway to Morocco, grows in contrasting environments, and displays considerable

68 phenotypic variation. The species displays a complex life cycle: reproduction takes place in the

69 Sargasso Sea, larvae (or leptocephali) are transported by ocean currents to European and North

70 African waters, where they experience their first metamorphosis to become glass eels. These

71 juveniles colonize continental waters and undergo progressive pigmentation changes to become

72 yellow eels. The growth phase lasts between two and 20 years depending upon the region and sex of

73 the eels (Vollestad 1992). At the end of this stage, yellow eels metamorphose again into silver eels,

74 which mature during the migration to their spawning area in the Sargasso Sea. The population is

75 panmictic, resulting in a homogeneous population, from a genetic viewpoint (Palm et al. 2009; Als et

76   al. 2011; Côté et al. 2013). This panmixia combined with a long and passive larval drift limit the

77   possibility of adaptation to local environments. However, spatial patterns of different life traits,

78   including growth rate (Daverat et al. 2012; Geffroy and Bardonnet 2012), sex (Helfman et al. 1987;

79   Tesch 2003; Davey and Jellyman 2005), length at maturity (Vollestad 1992; Oliveira 1999), and habitat

80   use (De Leo and Gatto 1995; Daverat et al. 2006; Edeline 2007) are observed and correlated with

81   environmental patterns.

82   Growth rates greatly vary depending on latitude, temperature, sex (Helfman et al. 1987) but

83   also on habitat characteristics (Cairns et al. 2009). Indeed, eel can settle in a wide range of habitats

84   (De Leo and Gatto 1995; Daverat et al. 2006; Geffroy and Bardonnet 2012) and faster growth is

85   observed in brackish waters than in freshwater (Daverat et al. 2012). Slower growth in freshwater

86   habitats is sometimes assumed to be compensated for by lower mortalities and Edeline (2007)

87   suggested that habitat choice could be the result of a conditional evolutionary stable strategy.

88   However, Cairns et al. (2009) questioned this assumption because they did not observe strong

89   variation in mortality rates between habitats. Spatial patterns were also observed with respect to sex

90   ratios, with female biased sex ratios in the upper part of river catchments (Tesch 2003) and in the

91   northern part of the distribution range (Helfman et al. 1987; Davey and Jellyman 2005). However, sex

92   is not determined at birth but is determined by environmental factors (Oliveira 2001; Davey and

93   Jellyman 2005; Geffroy and Bardonnet 2012). Population density also plays a role in this mechanism:

94   males are favored at high densities, whereas low densities favor females (Tesch 2003). This is

95   important because males and females have different life-history strategies (Helfman et al. 1987). The

96   reproductive success of a male does not vary with body size, and consequently, males are assumed

97   to follow a time-minimizing strategy, leaving continental waters as soon as they have enough energy

98   to migrate to the spawning grounds (Vollestad 1992). However, a female's reproductive success is

99   constrained by a trade-off between fecundity, which increases with length, and survival, which

100 decreases with length. Consequently, females are assumed to adopt a size-maximizing strategy

101   (Helfman et al. 1987). Strong differences in female length at silvering were observed among habitats

102   and latitudes (Oliveira 1999).

103   Because local adaptation is impossible, this raises two questions: (i) are those life-history

104   trait patterns resulting from an adaptive response to environmental heterogeneity, and (ii) which

105   adaptation mechanisms have been selected. Despite panmixia, previous researchers (Gagnaire et al.

106   2012; Ulrik et al. 2014; Pavey et al. 2015) have detected genetic differences correlated with

107   environmental gradients and assumed that those differences were reshuffled at each generation.

108   Common garden experiments have been used to test the respective contributions of genetic and

109   plastic mechanisms on phenotypic differences observed in glass eels found in distinct locations. The

110   results revealed genetic patterns related to geographic zones in American eels, whereas individual

111   growth rates had a genetic basis and could be sex-dependent (Côté et al. 2009, 2014, 2015). Building

112   on this, Boivin et al. (2015) studied the influence of salinity preferences and geographic origin on

113   habitat selection and growth in American eels, demonstrating genetic-based differences for growth

114   between glass eels from different origins. However, these experiments also confirmed the

115   contribution of phenotypic plasticity that allowed individuals to develop quick and effective

116   responses to environmental variability (Hutchings et al. 2007). Several traits have been proposed as

117   plastic: growth habitats (Daverat et al. 2006; Edeline 2007), growth rates (Geffroy and Bardonnet

118   2012), and length at silvering (Vollestad 1992). Understanding the adaptive mechanisms that explain

119   this diversity is crucial to environmental conservation and management (Brodersen and Seehausen

120   2014).

121   As a result of a decline observed since the 1980s, the European eel is now listed as critically

122   endangered in the IUCN Red List (Jacoby and Gollock 2014) and the European Commission enforced a

123   European Regulation, which requires a reduction in all sources of anthropogenic mortality (obstacles,

124   loss of habitat, fisheries, pollution, and global change) (Council of the European Union 2007).

125   However, those anthropogenic pressures are not uniformly distributed (Dekker 2003) and acts on

126   specific fractions of the stock isolated in river catchments (Dekker 2000), with heterogeneous life-

6

127   history traits because of the spatial phenotypic variability. This strong spatial heterogeneity of

128   anthropogenic pressures affecting the eel population in Europe combined with this spatial

129   phenotypic variability at both the distribution area and river catchment scales causes specific

130   challenges for management, because it impairs our ability to assess the effect of anthropogenic

131   pressures on the whole stock and to coordinate management actions (Dekker 2003, 2009).

132   Recently, a model called EvEel (evolutionary ecology-based model for eel) was developed to

133   explore the contribution of adaptive phenotypic plasticity in the emergence of observed phenotypic

134   patterns: sex ratio, length at silvering, and habitat use (Drouineau et al. 2014). Assuming fitness

135   maximization, the model was able to mimic most observed patterns at both river catchment and

136   distribution area scales. The result confirmed the probable role of adaptive phenotypic plasticity in

137   response to environmental variability. However, recent findings demonstrated the existence of

138   genetic differences in growth traits in a wide range of different habitats (Côté et al. 2009, 2014, 2015;

139   Boivin et al. 2015). Building on these new results, we developed GenEveel, a new version of EvEel,

140   which introduces a bimodal growth distribution (fast and slow growers) for individuals, as observed

141   by Côté et al. (2015), and considers phenotypic plasticity in life-history traits and demographic

142   attributes as in EvEel. Because individuals have different intrinsic growth and mortality rates, they

143   can be favored differently among environments, opening the door to conditional habitat selection. In

144   this study, we used GenEveel to test whether simultaneously considering genetically distinct

145   individuals and phenotypic plasticity improves model performance. Pattern orienting modelling was

146   used to detect the reproduced spatial patterns of EvEel and other patterns based on the distribution

147   of the different types of individuals.

148

3   Materials and methods

3.1   Model description

The model description follows the Overview, Design concepts, and Details (ODD) protocol (Grimm et al. 2006, 2010):

3.1.1 Overview

3.1.1.1 Purpose

GenEveel is a model based on a former model called EvEel (Drouineau et al. 2014), but includes a genetic component. It is an individual-based population model that predicts emergent life-history spatial patterns depending on adaptive mechanisms and environmental heterogeneity. Emergent patterns can later be compared to observed spatial patterns in freshwater life stages of European eels in order to (i) confirm that observed phenotypic patterns can plausibly result from adaptive responses to environmental heterogeneity, (ii) validate that phenotypic plasticity for length at silvering, sex determination, habitat choice, and genetic polymorphism (slow growers and fast growers) with conditional habitat selection can explain those patterns.

3.1.1.2 State variables and scales

Temporal scales: the model simulates a population generation. It has no *sensu stricto* time steps, but rather successive events: sex-determination and habitat selection, survival, and growth until maturation.

Entities and spatial scales: a Von Bertalanffy growth function is assumed for individual growth. Each individual i is characterized by an intrinsic Brody growth coefficient K_i and a natural mortality rate M_i. Based on Côté et al. (2015), who observed two clusters in growth rates, we build a simple quantitative-genetic model assuming that growth is coded for by a single gene with two variations. Therefore, we assumed that there are two types of individuals called (i) fast-growing

172   individuals for which $Ki = Kfast$ and $Mi = Mfast$ and (ii) slow-growing individuals for which $Ki = Kslow$

173   and $Mi = Mslow$. At the end of the simulation, individuals are characterized by a sex, length at

174   silvering, corresponding fecundity (if female), position in the river catchment, and survival rate until

175   silvering.

176   The river catchment environment was represented by a sequence of cells of the same size.

177   The first cell represents the river mouth, whereas the nth cell represents the source of the river.

178   Because it was observed that an individual grows faster downstream than upstream (Acou et al.

179   2003; Melià et al. 2006), we assumed that realized growth rate in a cell depends on both intrinsic

180   growth rate and position in the catchment (i.e., cell) (see submodel section). Realized natural

181   mortalities depend both on individual intrinsic mortality rates, position of the cell in the catchment,

182   and number of individuals in the catchment (to mimic density-dependent mortality).

183   **3.1.1.3 Process overview and scheduling**

184   The model has two main steps. In a first step, individuals select their growth habitat (a cell in

185   the catchment) and determine a sex (male or female) one after another (random order). To do that,

186   fitness is calculated for each combination of sex and cell (a quasi-Newton algorithm is used to

187   estimate the lengths at silvering that optimize female fitness in each cell). Individuals are assumed to

188   select the combination with highest fitness given the choices made by former individuals. Once this

189   step is finished (i.e., all individuals have a growth habitat and sex), using the quasi-Newton algorithm

190   we estimated the optimal length at silvering for all females (males have a constant length at silvering)

191   given the positions of fishes from step 1, and then compute corresponding survival rates until

192   silvering and fecundity determination (Fig. 1). The process mentioned above is defined by the

193   computer algorithm (Figure 2):

194   (1)   For each individual i:

195   -   For each cell x:

196   ·   Compute $\pi_m(x)$ given positions of individuals $\{1,...,i-1\}$

9

197   ·   Compute $\max\limits_{Ls_f} \pi_f\left(x, Ls_f\right)$ given positions of individuals *{1,...,i-1}*

198   -   Put individual and determine sex by selecting maximum values within $\max\limits_{Ls_f} \pi_f\left(x, Ls_f\right)$ and $\pi_m(x)$

199   (2)   For each individual i:

200   -   For each cell *x*:

201   ·   if sex(i) = male

202         $L_s(i) = L_{sm}$

203   ·   else

204         $L_s(i) = arg_L \max (\pi_f(x, L_{sf}))$ given positions of individuals *{1,...,n}*

205 where fitness is defined in equations 9 and 10 for females and males respectively.

3.1.2 Design concept

3.1.2.1 Basic principles

208   Consistent with life-history theory and optimal foraging theory, the model uses an

209 optimization approach in which individuals "respond to choices" so as to select and fix the adaptive

210 traits, maximizing their expected fitness given their environment (Parker and Maynard Smith 1990;

211 McNamara and Houston 1992; Giske et al. 1998; Railsback and Harvey 2013).

3.1.2.2 Emergence

213   Using the pattern-oriented modelling approach (Grimm and Railsback 2012), GenEveel

214 compares predicted spatial patterns with those observed in real river catchments. Five emergent

215 population spatial patterns were analyzed from the literature:

216 (i) higher density downstream than upstream

217 (ii) higher length at silvering upstream than downstream

218 (iii) male-biased sex ratio downstream and female-biased sex ratio upstream

219 (iv) more individuals characterized with the fast-growing genotype downstream than upstream,

220 which was mainly characterized by the slow-growing genotype

221 (v) the phenotypic response led to faster growth rate downstream than upstream.

222 **3.1.2.3 Adaptation**

223 Individuals have three adaptive traits: sex-determination, length at silvering for females, and

224 choice of growth habitat (cell in the grid). These traits are assumed to maximize the predicted

225 objective function (i.e., the individual fitness).

226 **3.1.2.4 Predictions**

227 We assumed that individuals could perfectly predict expected fitness given previous choices

228 and could make the most appropriate choices.

229 **3.1.2.5 Sensing**

230 In the model, individuals are able to "sense" fitness, which was a function of a density-

231 dependent mortality and growth rate. In the real world, temperature and density would probably be

232 the proximal cues because natural mortality and growth rates are strongly influenced by temperature

233 (Bevacqua et al. 2011; Daverat et al. 2012).

234 **3.1.2.6 Interaction**

235 Interactions occurred through growth habitat selection, sex determination, and density-

236 dependent mortality.

237 **3.1.2.7 Stochasticity**

238 Stochasticity occurred at two levels. First, individuals were randomly affected by a slow-

239 growing genotype (Pr = 0.5) or by a fast-growing genotype (Pr = 0.5). Then stochasticity occurred in

240 the order of individuals for step 1.

241 **3.1.2.8 Observations**

242   Five spatial patterns were computed at the end of the simulation:

243 (i) number of individuals per cell

244 (ii) mean length at silvering per cell

245 (iii) sex ratio (proportion of females) per cell

246 (iv) ratio of fast-growing genotype per cell

247 (v) phenotypic response of mean realized growth rate per cell.

248 These five patterns corresponded to five patterns available in the literature. Simulated patterns (i),

249 (iv), (v) was said to be consistent with the literature when a negative trend from downstream to

250 upstream was observed, whereas patterns (ii), (iii) were said to be consistent with the literature

251 when a positive trend was observed from downstream to upstream.

252 **3.1.3 Details**

253 **3.1.3.1 Initialization**

254   At the beginning of the simulation, the catchment was empty. N individuals were created and

255 attributed to the slow-growing or fast-growing genotype with probability 0.5 and had a length 7.5

256 cm. They had not yet entered the river catchment.

257 **3.1.3.2 Input data**

258   We tested the model using a reference simulation. Values of parameters were obtained from

259 the literature (Table 1). The outputs of the model were identified based on spatial patterns as

260 previously defined in *Observations*.

261   **3.1.3.3 Submodels**

262   Most of the submodels were similar to submodels from EvEel. Consequently, we provide

263   here only the novelties and the equations that are required for a better understanding of the model.

264   Further details are provided in Drouineau et al. (2014).

265   • Growth and silvering

266   Growth rate was assumed the outcome of an intrinsic Brody growth coefficient (Ki), which is

267   modulated by an environmental effect. This combination resulted in a phenotypic growth rate.

268   Within the river, growth rates were significantly faster downstream than upstream (even for the

269   same individual). Therefore, we assumed that individual i would have a growth rate $K(i, x)$ in cell x

270   given by:

271   (1) $K(i, x) = r_K \cdot K(i, n) + (K(i, 1) - r_K \cdot K(i, n)) \cdot \mathrm{cauchit}\left(\dfrac{x}{n}, \gamma_K\right)$

272   (2) $\mathrm{cauchit}(x, \gamma) = 1 - \dfrac{2}{\pi} \cdot \mathrm{atan}\left(\dfrac{x^2}{\gamma}\right)$

273   where r_k defined the ratio between upstream and downstream growth rate, $K(i, 1)$ is the growth rate

274   in cell 1, n is the total cells in the river catchment and *cauchit* was a mathematical function similar to

275   the sigmoid function, but which allowed asymmetrical patterns (by modifying the parameter γ) to

276   model, for example, a small brackish area in the downstream part of the catchment and a large

277   freshwater zone upstream.

278   Individual's growth was simulated by a Von Bertalanffy function:

279   (3) $L(t, i, x) = L_\infty \left[1 - e^{-K(i,x)(t - t_0)}\right]$

280   where $L(t, i, x)$ was the length at time t and L_∞ and $K(i, x)$, the Von Bertalanffy parameters in cell x for

281   individual i.

282   From this equation, we could calculate the time required to reach the length at silvering.

283   (4) $\mathrm{As}(i, x) = \dfrac{1}{K(i, x)} \cdot \log\left(\dfrac{L_\infty - Lg}{L_\infty - \mathrm{Ls}(i, x)}\right)$

284   where Lg was the length at recruitment and $Ls(i, x)$ was the length at silvering, which was constant

285   for males, and a fitness maximizing variable for females.

286   • Survival

287   Mortality rate was assumed the result of three factors: density-dependence, intrinsic growth

288   rate, and Mi modulated by an environmental effect. Because natural mortality was sometimes

289   assumed to be smaller upstream than downstream (Moriarty 2003; Daverat and Tomás 2006), we

290   assumed that the instantaneous natural mortality without density-dependence in cell x for individual

291   i, $M(i, x)$ was:

292   (5) $M(i, x) = r_M \cdot M(i, n) + (M(i, 1) - r_M \cdot M(i, n)) \cdot \text{cauchit}\left(\dfrac{x}{n}, \gamma_M\right)$

293   where r_m is the ratio between upstream and downstream instantaneous mortality rate and $M(i, 1)$

294   was the natural mortality in cell 1.

295   To account for the additional density-dependent mortality, we assumed that natural mortality

296   increased linearly with an intensity of density α as in EvEel:

297   (6) $M_d(i, x) = M(i, x) + N(i, x) \cdot \alpha$

298   where N was the number of competitors in cell x. An eel was assumed a competitor if it had an

299   intrinsic growth rate greater or equal to Ki. This corresponded to an asymmetric growth rate with

300   larger individuals harassing smaller individuals. The basis of this assumption was the intraspecific

301   competition, which leads to compete for limited resources between individuals of different sizes

302   (Francis 1983; Juanes et al. 2002).

303   Given equation (4) and this survival rate, we could calculate the probability of surviving until silvering

304   as:

305   (7) $p(i, x) = e^{-M_d(i, x) \cdot As(i, x)} = \left(\dfrac{L_\infty - Lg}{L_\infty - Ls(i, x)}\right)^{\dfrac{-M_d(i, x)}{K(i, x)}}$

306   • Fitness

307   In any optimization model, an important component is the computation of the fitness.

308   Because sexes adopt different life strategies, and following Drouineau et al. (2014), we assumed sex-

309   specific fitness functions. Males were known to adopt a time minimizing strategy (Helfman et al.

310   1987), with constant length at silvering. Therefore, male fitness was proportional to survival rate

311   until length at silvering. However, females follow a size-maximizing strategy in which length at

312   silvering was constrained by a trade-off between survival and fecundity (Helfman et al. 1987).

313   Consequently, we assumed that female fitness was the product of fecundity at an optimal length at

314   silvering (based on an allometric relationship, fecundity is assumed to be a power function of length)

315   multiplied by the probability of survival until this length at silvering. In the model, individuals were

316   assumed to determine their sex according to the relative potential male and female fitness. To make

317   fitness values comparable, we rescaled male fitness (which was the probability of survival) into an

318   expectation of egg production (the scale of female fitness). To do that, we multiplied the male

319   survival by a constant that would be similar to fertility. Hence, we had to specify a value for fertility

320   with an order of magnitude similar to fecundity. The first solution might be to fix the fertility value

321   equal to the fecundity of silver females having a length equal to male length at silvering. However,

322   with this solution, female fitness will always be greater (because females can optimize their length at

323   silvering). Consequently, fertility has to be slightly greater such that male fitness can be sometimes

324   be greater than female fitness (but not too much, to avoid male fitness always being superior). These

325   resulted in the following equations:

326   (8) $fecundity\left(L_{s_f}(i, x)\right) = \left(a_1 + a \cdot L_{s_f}(i, x)^b\right)$

327   where a1, a and b are the parameters of the allometric relationship linking fecundity and female

328   length at silvering $L_{sf}(i, x)$ (Andrello et al. 2011; Melia et al. 2006).

329   (9) $\pi_f(i, x) = fecundity\left(L_{s_f}(i, x)\right) \cdot \left[\dfrac{L_\infty - L_g}{L_\infty - L_{s_f}(i, x)}\right]^{\frac{-M_f(i, x)}{K(i, x)}}$

330   (10) $\pi_m(i, x) = fertility \cdot \left[\dfrac{L_\infty - L_g}{L_\infty - L_{s_m}(i, x)}\right]^{\frac{-M_m(i, x)}{K(i, x)}}$

3.2   Model exploration

3.2.1 Reference simulation

331

332

333   The reference simulation consisted of a simulation using parameter values in Table 1, i.e. the

334   best set of values found in the literature. After simulating this scenario, we analyzed the different

335   patterns. Mann-Kendall tests were implemented on each pattern to detect a monotonic upward or

336   downward trend of the variable of interest confirming the spatial patterns previously defined. The

337   correlation coefficient of this non-parametric test was denoted by τ.

3.2.2 Experimental design

338

339   Simulation design is a classical tool to explore complex models. Typically, the goal is to assess

340   the sensitivity of results to uncertain model parameters. We developed such an experimental design

341   to (i) assess the influence of uncertain parameters on the simulated patterns (Table 1) and (ii) derive

342   environmental and population dynamics for all the patterns that were correctly modelled.

343   Seventeen uncertain parameters were identified in the model (Table 1) and they were dispatched

344   into twelve groups: number of glass eel entering the catchment freshwater (N), parameters that

345   impact the male fitness (fertility and male length at silvering, L_{sm}), fast growing genotype ($K_{fast}(i, 1)$

346   and $M_{fast}(i, 1)$), slow-growing genotype ($K_{slow}(i, 1)$ and $M_{slow}(i, 1)$), proportion of individuals that grow

347   slowly (*propK*), intensity of density-dependence (α), cells of river catchment (n), regression

348   coefficient from fecundity at length (b), asymptotic length (L_∞), length at recruitment (L_g), ratio

349   between upstream and downstream instantaneous growth and mortality rates (r_k and r_m), and the

350   shape parameter of growth and mortality (γ_k and γ_m). Groups were composed of parameters that

351   have are assumed to influence the model in similar directions, a method called group-screening

352   (Kleijnen 1987). A low and high value was set for each parameter around the reference value, with

353   20% variation (Drouineau et al. 2006; Rougier et al. 2015), except for three sets of parameters:

354   *fertility* and L_{sm}(as a minimum value, *fertility* corresponded to the fecundity of a female with a length

16

355 at silvering equals to male length at silvering; otherwise, female fitness would always be superior to

356 male fitness), and growth genotypes (to avoid overlap between them), where the range of variation

357 was less. We then conducted a fractional factorial design of resolution V (2^{12-4} = 256 combinations).

358 This kind of orthogonal designs allows to explore main effects and first order interactions without

359 confusion. To account for model stochasticity, we conducted 10 replicates for each of the 256

360 combinations leading to 2560 simulations. The five patterns were calculated for each simulation

361 producing an output table with 2560 lines (one per simulation) and five columns containing the tau

362 value of the Mann-Kendall trend tests for each pattern (a negative tau value indicates a negative

363 trend from downstream to upstream while a positive tau indicates a positive trend from downstream

364 to upstream).

365

366   4   Results

367   *4.1   Reference simulation*

368   In the reference simulation, GenEveel mimicked the five spatial patterns at the catchment

369 scale (Fig. 3). Males were concentrated in the downstream section of the river where density was

370 higher (Helfman et al. 1987; Tesch 2003; Davey and Jellyman 2005). Fast growers preferentially

371 settled in downstream habitats, whereas slow growers tended to move upstream to avoid

372 competition (De Leo and Gatto 1995; Daverat et al. 2006, 2012; Drouineau et al. 2006; Edeline 2007;

373 Geffroy and Bardonnet 2012). Regarding mean length at silvering (for males and females), a smaller

374 size at maturity was simulated in the downstream section of the river, whereas larger lengths were

375 occurred gradually throughout the catchment (Vollestad 1992; Oliveira 1999).

376   The Mann-Kendall test confirmed that the five patterns were mimicked in the simulation.

377 More specifically, negative tau values confirmed a decreasing trend for density, ratio of fast growers

17

378   and mean realized growth rate; while positive tau values pointed to an increasing trend for ratio of

379   females and mean length at silvering (Table 2).

4.2   Model exploration

381   For each combination, the 10 replicates provided the same results, confirming that the

382   patterns were not sensitive to stochasticity.

383   Interestingly, 310 simulations produced only females while 640 simulations produced only

384   males. Simulations with only females corresponded to simulation where density-dependence α, L_∞

385   and the fecundity exponent b were simultaneously strong. Conversely, simulations with only males

386   corresponded to simulations with a low b and a low L_∞. With only one sex, it was not possible to

387   calculate a spatial trend in sex ratio and with only males, it was not possible to calculate a trend of

388   length at silvering.

389   Two questions were addressed here. In a first time, we compared the five patterns to see

390   which of those patterns were frequently mimicked and which were less frequently mimicked. Then,

391   we compared the sensitivity of the model to each group of parameters. To quantify this sensitivity to

392   a group of parameters values, we compared the number of simulations that reproduce a given

393   pattern when the group had modality (-) with the number of simulations and when the group had

394   modality (+). A strong discrepancy indicated a high sensitivity to the group of parameters.

395   The Mann-Kendall tests of spatial patterns confirmed that the simulated patterns of

396   abundance, ratio of fast growers, and mean realized growth rate were consistent with the literature

397   in each of the 2560 combinations (Table 3). This result indicates that these model outputs do not

398   depend on parameters values in the parameter space considered. Consequently, the assumptions

399   about asymmetrical density-dependence and growth genotypes were enough to simulate catchment

400   colonization.

401   Regarding length at silvering pattern, patterns were consistent in 1300 simulations of the

402   1920 simulations for which it was possible to calculate a pattern (Table 3, Fig. 4 for several examples).

403   This meant that, in situations where some females were produced, the pattern was consistent in

404   about 2/3 of the simulations. Length at silvering pattern appeared to be sensitive to most of the

405   parameters. The two most important were L_∞ and b: consistent pattern were much more frequent

406   with a modality (+) (respectively 990 and 940 simulations) for these two parameters than with

407   modality (-) (respectively 310 and 360 simulations). This is not surprising since with modality (-) for

408   those parameters, the model produced only males in 640 simulations. Two other groups of

409   parameters had a strong influence: male fertility/ male length at silvering and density-dependence.

410   Consistent patterns were more frequent with low male fertility and length at silvering (800 with

411   modality (-) vs 500 with modality (+)), and with limited density dependence (810 with modality (-) vs

412   490 with modality (+)).

413   For the female ratio pattern, 130 simulations produced consistent patterns over the 1610

414   simulations for which it was possible to calculate a pattern (Table 3). This pattern was mostly

415   sensitive to four groups of parameters which correspond to the four most influential groups for the

416   pattern of length at silvering. Patterns were consistent only when male fertility/length at silvering

417   had modality (-) whereas Kslow/Mslow had modality (+). Moreover, consistent patterns were more

418   frequent when L_∞ had a modality (-) and b a modality (+).

419   On the whole, 130 of the 2560 combinations produced results which were consistent for all

420   the five patterns (Table 4, Fig. 4 and Table S1). These 130 simulations corresponded exactly to the

421   130 simulations that produced consistent sex ratio patterns, demonstrating that this last pattern was

422   the more constraining (Fig. 5). Consequently, the interpretation regarding sensitive parameters was

423   similar.

424   To make a summary of those results: in situations where females' fitness was favored

425   because of a strong L_∞ or a strong b, i.e. a high fecundity, the model produced only females.

426   Conversely, when females were too penalised, model produced only males. Therefore, an equilibrium

427   was required between males and females fitnesses to mimic all patterns. The patterns in length at

428   silvering and sex ratio were the two most constraining patterns and were mainly sensitive to four

429   groups of patterns. These groups of parameters set the equilibrium between males and females

430   fitnesses (male fertility and length at silvering, b and L_∞) and the advantages between slow and fast

431   growers. Density-dependence was also important regarding the pattern on length at silvering. We

432   can observed that the five patterns were consistent mostly when slow growers and females were not

433   too penalized with respect to males and fast-growers.

434   Some of the patterns were indeed very constrained by model assumptions so it is hardly

435   surprising that they were mimicked by the model. For example, our constraints on mortality and

436   growth really constrained the distribution of fishes and probably the pattern of realized growth rates

437   in the catchment. However, those constraints were based on various observations in the literature

438   that have rarely been considered together to see if they make sense in a context of adaptive

439   response. We do not specify any constraints on the sex ratio, length at maturity and relationships

440   between sex ratio and slow/fast growers. Those results are really emerging patterns that are

441   consistent with the literature.

442

5   Discussion

5.1 *Adaptation to environmental variability: phenotypic plasticity and genetic polymorphism of European eel*

446   The European eels, and more generally, temperate eels, display fascinating characteristics:

447   catadromy with a long larval drift, large distribution area with contrasted growth habitats, panmixia,

448   and strong phenotypic and tactic variability at different spatial scales. Consequently, this species is

449   relevant to explore adaptive mechanisms to environmental variability. Phenotypic plasticity has been

450   proposed as one such mechanism because of random mating and larval dispersal that prevent local

451   selection pressures to generate habitat-specific adaptations, or local adaptation, from one generation

452   to the next. Drouineau et al. (2014) developed the first model to explore the major role of

453   phenotypic plasticity in both life-history traits and tactical choices as an adaptive response to

454   spatially structured environments and density dependence. However, recently Gagnaire et al. (2012),

455   Pujolar et al. (2014), Boivin et al. (2015), Côté et al. (2015) and Pavey et al. (2015) demonstrated the

456   existence of genetic differences correlated with the environment, suggesting that part of the

457   observed phenotypic variability had a genetic basis.

458   Based on the approach developed by Drouineau et al. (2014), the objective of this study was

459   to propose a model based on life-history theory and optimal foraging theory to explore the role of

460   both adaptive phenotypic plasticity and genetic polymorphism with genetic-dependent habitat

461   selection, in the emergence of phenotypic patterns. To that end, we used a pattern-oriented

462   modelling approach, as developed by Grimm et al. (1996). This kind of approach compared field

463   observed patterns to simulated patterns and postulated that those patterns are similar, the model is

464   likely to contain the mechanisms generating these patterns.

465   *5.2   In which conditions were the patterns mimicked?*

466   Similarly to Eveel, a main limitation of our approach was that it was based on a simulation

467   model with a pattern-oriented approach. Consequently, our results demonstrated that our

468   assumptions were plausible, but did not demonstrate that they were correct. Such a demonstration

469   would require demonstrating underlying mechanisms, for example by conducting complementary

470   controlled experiments.

471   We built a full experimental design to explore the model. This type of approach is classical in

472   complex model exploration (de Castro et al. 2001; Faivre et al. 2013). For example, in the context of

473   sensitivity analysis of complex simulation models (Drouineau et al. 2006). Our exploration goals were

474   to generate simulations from the parameter space and analyze the qualitative differences in the

475   model output to (i) study the impact of parameters on the model output, (ii) determine which

476   parameters were the most important, and (iii) identify the combinations of parameters required to

477   mimic all observed spatial patterns. In this study, 17 parameters grouped in 12 set of parameters,

478   were chosen to define the region of the parameter space where all spatial patterns were reproduced.

479   To assess the influence of stochasticity, we made 10 replicates per combination. This can

480   appear limited, however, it was impossible to increase the number of simulations and we preferred

481   to have a better exploration of uncertainty due to uncertain parameters rather than on stochasticity

482   which is rather limited in our model. Stochasticity occurs during the initialization process when

483   randomly building slow or fast value with a given probability. This corresponds to a binomial

484   distribution which has, given the large number of individuals, a very small variance. Stochasticity also

485   occurs in the order of individuals for step 1, but this is closely linked to the previous process and

486   consequently also has a limited variability. This limited effect of stochasticity was confirmed by our

487   results since patterns per combination were always consistent among replicates (Fig. 4 and 5).

488   One hundred thirty simulations among the 2560 mimicked the five spatial patterns. The

489   fourth pattern stated that fast growers and slow growers had different spatial distributions. Fulfilling

490   this pattern demonstrated that genetically different individuals have different habitat selection

491   strategies to maximize their respective fitnesses. Consequently, fulfilling the five patterns suggested

492   that, at least in certain conditions, genotype-dependent habitat selection and phenotypic plasticity

493   could explain observed phenotypic patterns. The level of sensitivity was variable among groups of

494   parameters, but four main groups of parameters were crucial: males' fertility and length at silvering,

495   growth and mortality rates of slow growers, fecundity, and L_∞. Density-dependence was also an

496   important parameter regarding length at silvering. In summary, the patterns were mimicked in

497   simulations with dominants and dominated but when dominated individuals, mainly females, were

498   not too penalized with respect to dominants, mainly males.

499   Regarding the spatial patterns, higher density, higher proportions of fast growers, and faster

500   growth rates in downstream regions were mimicked for all combinations of parameters. This

501   suggested that in the range of variation considered, none of the parameters had effects on model

502   outputs. This probably means that the gradient in environmental conditions and the population

503   dynamics in the model were sufficient to reproduce these patterns, regardless of the competitive

504   advantage of fast growers with respect to slow growers, confirming that phenotypic plasticity plays

505   an important role in environmentally induced changes in life-history traits and demographic

506   attributes. Concerning the two other patterns (sex ratio and length at silvering), additional

507   hypotheses are needed regarding competition and genetic polymorphism. They were fulfilled in

508   conditions of weak competition and when growth differences were not too strong between the two

509   genotypes.

5.3   Consequences of intra-specific competition

511   In our model, we assumed the existence of asymmetrical density dependence between fast

512   and slow growers. We assumed that smaller individuals would avoid engaging in competition with

513   larger ones (regardless of sex) and would consequently be more affected by density dependence.

514   This assumption seems ecologically realistic. Asymmetrical density dependence has been observed in

515   plants (Weiner 1990), insects (Varley et al. 1973), and fish (DingsØr et al. 2007). Intraspecific

516   competition is a very common mechanism of density dependence, favoring large body size in fishes

517   (Francis 1983; Juanes et al. 2002). In anguillid eels, this may be manifested through agonistic

518   interactions (Knights 1987; Bardonnet et al. 2005), including cannibalism (Edeline and Elie 2004).

519   Such behaviors have been observed in yellow eels under artificial rearing conditions (Peters et al.

520   1980; Degani and Levanon 1983; Knights 1987).

521   We modelled this asymmetric competition by specifying different levels of density-

522   dependent mortality for slow and fast growers. Interestingly, the spatial patterns were still

523   reproduced when setting these parameters to a similar value (not presented here). Indeed, even with

524   similar intensity of density dependence, slow growers needed more time to reach their length at

525   silvering and consequently, suffered competition longer. Thus, even if competition has the same

526   impact on instantaneous mortality rates of slow and fast-growers, density dependence produces

527   asymmetric impacts on their respective fitness. In EvEel, Drouineau et al. (2014) assumed the

528   existence of asymmetric competition between males and females, with females being more affected

529   by competition. Interestingly, we observed in our results that females had a higher proportion of

530   slow growers than males. This means that the gender-based asymmetry proposed by Drouineau et al.

531   (2014) may be an indirect result of an asymmetry between two genetically distinct types of

532   individuals with respect to growth.

533   The asymmetric competition implies that fitness of individuals having a given growth

534   genotype depends on the number of individuals having the other growth genotype, which may lead

535   to frequency-dependent selection (Heino et al. 1998). This has several implications. In the model, we

536   assumed that individual fitness corresponded to the lifetime reproductive success called R0, and that

537   this fitness is maximized. However, in a frequency-dependent selection context (i) natural selection

538   does not necessarily lead in fitness maximization (Mylius and Diekmann 1995; Metz et al. 2008), and

539   (ii) fitness may need to be defined as an invasion criterion (Metz et al. 1992). Even when fitness

540   maximization applies, r, the population growth rate, may be a more appropriate measure of fitness

541   than R0 depending on how density-dependence acts (Mylius and Diekmann 1995). To ensure that

542   our assumptions about fitness definition and maximization were valid would require a multi-

543   generational model at the scale of the population distribution area. This would allow computing

544   fitness for the whole life-cycle across all potential habitat types of the distribution area while

545   accounting for population structure in terms of genotypes or clusters. At this point, it would be

546   interesting to explore the heritability of the different traits and the intra-generational spatially

547   varying selection, a mechanism suggested by the SNP differences according to latitude (Pujolar et al.

548   2011; Gagnaire et al. 2012; Ulrik et al. 2014).

549   This was not possible because of difficulties to develop a whole life-cycle model. More

550   specifically, the fractal dimension of the eel population makes it very difficult to develop a population

551   dynamics model for the continental phase at the distribution area scale. Moreover, such a model

552   would require the use of stock-recruitment relationships, which is very difficult for the European eels

553   because of insufficient data, long larval drift, and different recruitment trends through the

554   distribution area. In this context, we had to use intra-generational model and a R0 fitness function,

555   restricted to a single catchment and a portion of the whole life-cycle, and to postulate that this R0

556   was maximized.

557   *5.4   **Reinterpreting the time-minimizing and size-maximizing strategies***

558   To summarize the results for combinations of parameters that mimicked observed patterns,

559   we observed a high proportion of individuals, mainly fast growers, in the downstream environment,

560   which corresponded to marine or brackish water. These individuals were mainly males with a

561   constant length at silvering. In upstream areas, we found mainly slow growers, primarily females with

562   higher length at silvering. This can aid in the reinterpretation of gender difference in life tactics (i.e.,

563   males with a time-maximizing strategy and females with a size-maximizing strategy). Our results

564   suggest that these tactics were possibly based on the existence of two genotypes for growth. Fast

565   growers grow fast but suffer higher mortality (because they inhabit downstream habitats with higher

566   mortality and density); a time-minimizing strategy is suitable for them. Slow growers grow slowly but

567   suffer lower mortality, consequently they can stay longer in continental habitats, and a size-

568   maximizing strategy is suitable for them.

569   Another interesting question is whether cues are used by individuals to select their growth

570   habitat. In the model, individuals were omnipotent and omniscient: they were able to assess the

571   potential fitness in each cell and move in the most suitable cell. This would mean that they were able

572   to assess the natural mortality, growth rate, and density in each cell. Drouineau et al. (2014)

573   suggested that temperature might be one of the main proximal cue used by individuals to assess the

574   suitability. Regarding density-dependence, reaction to aggressiveness (Geffroy and Bardonnet, 2012)

575   or cons-specific odors (Schmucker et al. 2016) were observed on growth and propensity to migrate.

576   Vélez-Espino and Koops (2010) also revealed temperature as main factor explaining variation in life-

577   history traits. Our model suggested that density in various habitats was also probably a main cue,

578   especially for slow growers, which tended to minimize competition.

579   *5.5   Perspectives*

580   **5.5.1 Exploring conditions in which phenotypic plasticity is adaptive**

581   It has been demonstrated that phenotypic plasticity allows short-term adaptation to

582   environmental heterogeneity for many species (Schlichting 1986; Sultan 1987; Scheiner 1993;

583   Pigliucci 2005). However, the fitness gain arising from phenotypic plasticity should overcome its cost

584   to be selected. This last point has not been demonstrated for eels. One possibility would be to

585   simulate the evolution of a plastic reaction norm, for example length at silvering, close to the model

586   developed by Marty et al. (2011). Following Ernande et al. (2004) and based on adaptive dynamics

587   models (Mylius and Diekmann 1995), it would be interesting to explore in which environmental and

588   density-dependence conditions, phenotypic plasticity may be selected as an adaptive mechanism

589   despite its costs, and if plasticity is still adaptive in a context of low densities after a population

590   collapse.

591   **5.5.2 Assessing the impact of anthropogenic pressures at the distribution**

592   **area scale**

593   Another perspective is to assess the impact of anthropogenic pressures on eel populations.

594   Drouineau et al. (2014) mentioned that, because of phenotypic plasticity, anthropogenic pressures

595   are not only a source of mortality, but may also affect sex ratio or mean length at silvering. The

596   existence of two genotypes for growth suggests that anthropogenic activities may act as selective

597   forces. Recently, Podgorniak et al. (2015) demonstrated that human-induced obstacles to migration

598   could act as an evolutionary pressure. Concerning this, Boulenger et al. (2016) highlighted that

599   human pressures impact survival, leading to different life-history strategies.

600

601   To conclude, our model provided new insights on eel adaptive mechanisms to heterogeneous

602   environments. Phenotypic plasticity and genotype-dependent habitat selection are two types of

603   mechanisms that can explain the patterns in life-history traits observed in natural environments at

604   the river catchment scale. A better understanding of these mechanisms is crucial to interpret the

605   observations made in the environment, the effects of anthropogenic pressures on the population,

606   and to understand if eels are still adapted in the context of depleted population size and climate

607   change.

608

6   Acknowledgements

613

7   References

615   Acou, A., Lefebvre, F., Contournet, P., Poizat, G., Panfili, J., and Crivelli, A.J. 2003. Silvering of female
616   eels (*Anguilla anguilla*) in two sub-populations of the Rhone Delta. Bull. Fr. Pêche Piscic. 368:
617   55–68.

618   Als, T.D., Hansen, M.M., Maes, G.E., Castonguay, M., Riemann, L., Aarestrup, K., Munk, P., Sparholt,
619   H., Hanel, R., and Bernatchez, L. 2011. All roads lead to home: panmixia of European eel in
620   the Sargasso Sea. Mol. Ecol. **20**(7): 1333–1346. doi:10.1111/j.1365-294X.2011.05011.x.

621   Andrello, M., Bevacqua, D., Maes, G.E., and De Leo, G.A. 2011. An integrated genetic-demographic
622   model to unravel the origin of genetic structure in European eel (*Anguilla anguilla* L.):
623   Genetic-demographic model for the European eel. Evol. Appl. **4**(4): 517–533.
624   doi:10.1111/j.1752-4571.2010.00167.x.

625   Bardonnet, A., Rigaud, C., and Labonne, J. 2005. Etude expérimentale des comportements de civelles
626   d'*Anguilla anguilla* L. influence de la densité et de la disponibilité en abris. Bull. Fr. Pêche
627   Piscic. **378**–**379**: 47–65.

628   Bevacqua, D., Melià, P., De Leo, G.A., and Gatto, M. 2011. Intra-specific scaling of natural mortality in
629   fish: the paradigmatic case of the European eel. Oecologia **165**(2): 333–339.
630   doi:10.1007/s00442-010-1727-9.

631   Boivin, B., Castonguay, M., Audet, C., Pavey, S.A., Dionne, M., and Bernatchez, L. 2015. How does
632   salinity influence habitat selection and growth in juvenile American eels *Anguilla rostrata*?:
633   salinity preference in *Anguilla rostrata* glass eels. J. Fish Biol. **86**(2): 765–784.
634   doi:10.1111/jfb.12604.

635   Boulenger, C., Acou, A., Gimenez, O., Charrier, F., Tremblay, J., and Feunteun, E. 2016. Factors
636   determining survival of European eels in two unexploited sub-populations. Freshw. Biol.
637   **61**(6): 947–962. doi:10.1111/fwb.12759.

638   Brodersen, J., and Seehausen, O. 2014. Why evolutionary biologists should get seriously involved in
639   ecological monitoring and applied biodiversity assessment programs. Evol. Appl. **7**(9): 968–
640   983. doi:10.1111/eva.12215.

641   Cairns, D.K., Secor, D.A., Morrison, W.E., and Hallett, J.A. 2009. Salinity-linked growth in anguillid eels
642   and the paradox of temperate-zone catadromy. J. Fish Biol. **74**(9): 2094–2114.
643   doi:10.1111/j.1095-8649.2009.02290.x.

644   de Castro, L.A.B., Petrere Jr., M., and Comune, A.E. 2001. Sensitivity of the BEAM4 fisheries
645   bioeconomic model to the main biological input parameters. Ecol. Model. **141**(1–3): 53–66.
646   doi:10.1016/S0304-3800(01)00241-1.

647   Clark, C.W. 1993. Dynamic Models of Behavior: An extension of Life-history Theory. Tree **8**(6): 205–
648   209.

649   Côté, C.L., Castonguay, M., Kalujnaia, M., Cramb, G., and Bernatchez, L. 2014. In absence of local
650   adaptation, plasticity and spatially varying selection rule: a view from genomic reaction
651   norms in a panmictic species (*Anguilla rostrata*). BMC Genomics **15**(1): 403.
652   doi:10.1186/1471-2164-15-403.

653   Côté, C.L., Castonguay, M., Verreault, G., and Bernatchez, L. 2009. Differential effects of origin and
654   salinity rearing conditions on growth of glass eels of the American eel *Anguilla rostrata* :
655   implications for stocking programmes. J. Fish Biol. **74**(9): 1934–1948. doi:10.1111/j.1095-
656   8649.2009.02291.x.

657   Côté, C.L., Gagnaire, P.-A., Bourret, V., Verreault, G., Castonguay, M., and Bernatchez, L. 2013.
658   Population genetics of the American eel (*Anguilla rostrata*): $F_{ST} = 0$ and North Atlantic
659   Oscillation effects on demographic fluctuations of a panmictic species. Mol. Ecol. **22**(7):
660   1763–1776. doi:10.1111/mec.12142.

661   Côté, C.L., Pavey, S.A., Stacey, J.A., Pratt, T.C., Castonguay, M., Audet, C., and Bernatchez, L. 2015.
662   Growth, Female Size, and Sex Ratio Variability in American Eel of Different Origins in Both
663   Controlled Conditions and the Wild: Implications for Stocking Programs. Trans. Am. Fish. Soc.
664   **144**(2): 246–257. doi:10.1080/00028487.2014.975841.

665   Council of the European Union. 2007. Council Regulation (EC) No 1100/2007 of 18 September 2007
666   establishing measures for the recovery of the stock of European eel. Brussels: 7pp.

667   Daverat, F., Beaulaton, L., Poole, R., Lambert, P., Wickström, H., Andersson, J., Aprahamian, M.,
668   Hizem, B., Elie, P., Yalçın-Özdilek, S., and Gumus, A. 2012. One century of eel growth: changes
669   and implications. Ecol. Freshw. Fish **21**(3): 325–336. doi:10.1111/j.1600-0633.2011.00541.x.

670   Daverat, F., Limburg, K.E., Thibault, I., Shiao, J.-C., Dodson, J.J., Caron, F., Tzeng, W.-N., Iizuka, Y., and
671   Wickstrom, H. 2006. Phenotypic plasticity of habitat use by three temperate eel species,
672   *Anguilla anguilla*, *A. japonica* and *A. rostrata*. Mar. Ecol. Prog. Ser. **308**: 231–241.

673   Daverat, F., and Tomás, J. 2006. Tactics and demographic attributes in the European eel *Anguilla*
674   *anguilla* in the Gironde watershed, SW France. Mar. Ecol.-Prog. Ser. **307**: p–247.

675   Davey, A.J.H., and Jellyman, D.J. 2005. Sex Determination in Freshwater Eels and Management
676   Options for Manipulation of Sex. Rev. Fish Biol. Fish. **15**(1–2): 37–52. doi:10.1007/s11160-
677   005-7431-x.

678   De Leo, G.A., and Gatto, M. 1995. A size and age-structured model of the European eel (*Anguilla*
679   *anguilla* L.). Can. J. Fish. Aquat. Sci. **52**: 1351–1367.

680   Degani, G., and Levanon, D. 1983. The influence of low density on food adaptation, cannibalism and
681   growth of eels (*Anguilla anguilla* (L.)). Bamidgeh **35**: 53–60.

682   Dekker, W. 1998. Long-term trends in the glass eels immigrating at Den Oever, The Netherlands. Bull.
683   Fr. Pêche Piscic. (349): 199–214. doi:10.1051/kmae:1998045.

684   Dekker, W. 2000. The fractal geometry of the European eel stock. ICES J. Mar. Sci. **57**(1): 109–121.
685   doi:10.1006/jmsc.1999.0562.

686   Dekker, W. 2003. Status of the European Eel Stock and Fisheries. *In* Eel Biology. *Edited by* K. Aida, K.
687   Tsukamoto, and K. Yamauchi. Springer Japan. pp. 237–254.

688   Dekker, W. 2009. Worldwide decline of eel resources necessitates immediate action.

689   Desaunay, Y., and Guerault, D. 1997. Seasonal and long-term changes in biometrics of eel larvae: a
690   possible relationship between recruitment variation and North Atlantic ecosystem
691   productivity. J. Fish Biol. **51**(sA): 317–339.

692   Desaunay, Y., Lecomte-Finiger, R., and Guérault, D. 2012. Mean age and migration patterns of
693   *Anguilla anguilla* (L.) glass eels from three French estuaries (Somme, Vilaine and Adour
694   Rivers). Arch. Pol. Fish. **20**(3). doi:10.2478/v10086-012-0023-1.

695   DingsØr, G.E., Ciannelli, L., Chan, K.-S., Ottersen, G., and Stenseth, N.C. 2007. Density dependence
696   and density independence during the early life stages of four marine fish stocks. Ecology
697   **88**(3): 625–634.

698   Drouineau, H., Mahévas, S., Pelletier, D., and Beliaeff, B. 2006. Assessing the impact of different
699   management options using ISIS-Fish: the French *Merluccius merluccius – Nephrops*
700   *norvegicus* mixed fishery of the Bay of Biscay. Aquat. Living Resour. **19**(1): 15–29.
701   doi:10.1051/alr:2006002.

702   Drouineau, H., Rigaud, C., Daverat, F. and Lambert, P. 2014. EvEel (evolutionary ecology-based model
703   for eel): a model to explore the role of phenotypic plasticity as an adaptive response of three
704   temperate eels to spatially structured environments. Can. J. Fish. Aquat. Sci. **71**(10): 1561–
705   1571. doi:10.1139/cjfas-2014-0090.

706   Edeline, E. 2007. Adaptive phenotypic plasticity of eel diadromy. Mar. Ecol. Prog. Ser. **341**: 229–232.

707   Edeline, E., and Elie, P. 2004. Is salinity choice related to growth in juvenile eel *Anguilla anguilla*?
708   Cybium **28**: 77–82.

709   Ernande, B., Dieckmann, U., and Heino, M. 2004. Adaptive changes in harvested populations:
710   plasticity and evolution of age and size at maturation. Proc. R. Soc. Lond. B Biol. Sci.
711   **271**(1537): 415–423.

712   Faivre, R., Iooss, B., Mahévas, S., Makowski, D., and Monod, H. 2013. Analyse de sensibilité et
713   exploration de modèles. Editions Quae.

714   Francis, R.C. 1983. Experiential effects on agonistic behavior in the paradise fish, *Macropodus*
715   *opercularis*. Behaviour **85**(3): 292–313.

716   Gagnaire, P.-A., Normandeau, E., Cote, C., Moller Hansen, M., and Bernatchez, L. 2012. The Genetic
717   Consequences of Spatially Varying Selection in the Panmictic American Eel (*Anguilla*
718   *rostrata*). Genetics **190**(2): 725–736. doi:10.1534/genetics.111.134825.

719   Geffroy, B., and Bardonnet, A. 2012. Differential effects of behaviour, propensity to migrate and
720   recruitment season on glass eels and elvers' growing performance: Young eel behaviour and
721   growth pattern. Ecol. Freshw. Fish **21**(3): 469–482. doi:10.1111/j.1600-0633.2012.00566.x.

722   Giske, J., Huse, G., and Fiksen, O. 1998. Modelling spatial dynamics of fish. Rev. Fish Biol. Fish. **8**: 57–
723   91. doi:10.1023/A:1008864517488.

724   Gotthard, K., and Nylin, S. 1995. Adaptive plasticity and plasticity as an adaptation: a selective review
725   of plasticity in animal morphology and life-history. Oikos **74**(1): 3–17. doi:10.2307/3545669.

726   Grimm, V., Berger, U., Bastiansen, F., Eliassen, S., Ginot, V., Giske, J., Goss-Custard, J., Grand, T., Heinz,
727   S.K., Huse, G., Huth, A., Jepsen, J.U., Jørgensen, C., Mooij, W.M., Müller, B., Pe'er, G., Piou, C.,
728   Railsback, S.F., Robbins, A.M., Robbins, M.M., Rossmanith, E., Rüger, N., Strand, E., Souissi, S.,

729   Stillman, R.A., Vabø, R., Visser, U., and DeAngelis, D.L. 2006. A standard protocol for
730   describing individual-based and agent-based models. Ecol. Model. **198**(1–2): 115–126.
731   doi:10.1016/j.ecolmodel.2006.04.023.

732   Grimm, V., Berger, U., DeAngelis, D.L., Polhill, J.G., Giske, J., and Railsback, S.F. 2010. The ODD
733   protocol: A review and first update. Ecol. Model. **221**(23): 2760–2768.
734   doi:10.1016/j.ecolmodel.2010.08.019.

735   Grimm, V., Frank, K., Jeltsch, F., Brandl, R., Uchmanski, J., and Wissel, C. 1996. Pattern-oriented
736   modelling in population ecology. Sci. Total Environ. **183**: 155–166.

737   Grimm, V., and Railsback, S.F. 2012. Pattern-oriented modelling: a "multi-scope" for predictive
738   systems ecology. Philos. Trans. R. Soc. B Biol. Sci. **367**(1586): 298–310.
739   doi:10.1098/rstb.2011.0180.

740   Heino, M., Metz, J.A.J., and Kaitala, V. (1998). The enigma of frequency-dependent selection. Trends
741   Ecol. Evol. (13): 367–370.

742   Helfman, G.S., Facey, D.E., Stanton Hales, L., and Bozeman, E.L. 1987. Reproductive Ecology of the
743   American eel. Am. Fish Soc. Symp. **1**: 42–56.

744   Hutchings, J.A., Swain, D.P., Rowe, S., Eddington, J.D., Puvanendran, V., and Brown, J.A. 2007. Genetic
745   variation in life-history reaction norms in a marine fish. Proc. R. Soc. B Biol. Sci. **274**(1619):
746   1693–1699. doi:10.1098/rspb.2007.0263.

747   Jacoby, D., and Gollock, M. 2014. *Anguilla anguilla*. The IUCN Red List of Threatened Species.
748   Available from http://www.iucnredlist.org/details/60344/0.

749   Juanes, F., Buckel, J.A., and Scharf, F.S. 2002. Feeding ecology of piscivorous fishes. *In* Handbook of
750   fish biology and fisheries, Blackwell. Paul J.B. Hart and John D. Reynolds, UK. pp. 267–283.

751   Kawecki, T.J., and Ebert, D. 2004. Conceptual issues in local adaptation. Ecol. Lett. **7**(12): 1225–1241.
752   doi:10.1111/j.1461-0248.2004.00684.x.

753   Kleijnen, J.P.C. 1987. Statistical Tools for Simulation Practitioners. Marcel Dekker, Inc., New York, NY,
754   USA.

755   Knights, B. 1987. Agonistic behaviour and growth in the European eel, *Anguilla anguilla* L., in relation
756   to warm-water aquaculture. J. Fish Biol. **31**(2): 265–276.

757   Levins, R. 1963. Theory of fitness in a heterogeneous environment. II. Developmental flexibility and
758   niche selection. Am. Nat. **97**(893): 75–90. doi:10.1086/ 282258.

759   Marty, L., Dieckmann, U., Rochet, M.-J., and Ernande, B. 2011. Impact of Environmental Covariation
760   in Growth and Mortality on Evolving Maturation Reaction Norms. Am. Nat. **177**(4): E98–
761   E118. doi:10.1086/658988.

762 McNamara, J.M., and Houston, A.I. 1992. State-dependent life-history theory and its implications for

763   optimal clutch size. Evol. Ecol. **6**(2): 170–185. doi:10.1007/BF02270710.

764 Melià, P., Bevacqua, D., Crivelli, A.J., De Leo, G.A., Panfili, J., and Gatto, M. 2006. Age and growth of

765   *Anguilla anguilla* in the Camargue lagoons. J. Fish Biol. **68**: 876–890. doi:10.1111/j.1095-

766   8649.2006.00975.x.

767 Metz, J.A.J., Mylius, S.D., and Diekmann, O. 2008. When does evolution optimize? Evol. Ecol. Res.

768   **10**(5): 629–654.

769 Metz, J.A.J., Nisbet, R.M., and Geritz, S.A.H. 1992. How should we define "fitness" for general

770   ecological scenarios? Trends Ecol. Evol. **7**(6): 198–202.

771 Moriarty, C. 2003. The eel. *In* Eel Biology. Springer Japan, Tokyo. pp. 89–105.

772 Mylius, S.D., and Diekmann, O. 1995. On Evolutionarily Stable Life Histories, Optimization and the

773   Need to Be Specific about Density Dependence. Oikos **74**(2): 218–224.

774 Oliveira, K. 1999. Life-history characteristics and strategies of the American eel, *Anguilla rostrata*.

775   Can. J. Fish. Aquat. Sci. **56**(5): 795–802.

776 Oliveira, K. 2001. Regional variation and the effect of lake: river area on sex distribution of American

777   eels. J. Fish Biol. **58**(4): 943–952. doi:10.1006/jfbi.2000.1503.

778 Palm, S., Dannewitz, J., Prestegaard, T., and Wickström, H. 2009. Panmixia in European eel revisited:

779   no genetic difference between maturing adults from southern and northern Europe.

780   Heredity **103**(1): 82–89.

781 Parker, G.A., and Maynard Smith, J. 1990. Optimality theory in evolutionary biology. Nature **348**: 27–

782   33.

783 Pavey, S.A., Gaudin, J., Normandeau, E., Dionne, M., Castonguay, M., Audet, C., and Bernatchez, L.

784   2015. RAD Sequencing Highlights Polygenic Discrimination of Habitat Ecotypes in the

785   Panmictic American Eel. Curr. Biol. **25**(12): 1666–1671. doi:10.1016/j.cub.2015.04.062.

786 Peters, G., Delventhal, H., and Klinger, H. 1980. Physiological and Morphological Effects of Social

787   Stress on the Eel, *Anguilla anguilla* L. *In* Fish Diseases. *Edited by* D.W. Ahne. Springer Berlin

788   Heidelberg. pp. 225–227.

789 Pigliucci, M. 2005. Evolution of phenotypic plasticity: Where are we going now? Trends Ecol. Evol.

790   **20**(9): 481–486. doi:10.1016/j.tree.2005.06.001.

791 Podgorniak, T., Angelini, A., Blanchet, S., de Oliveira, E., Pierron, F., and Daverat, F. 2015. Climbing

792   experience in glass eels: A cognitive task or a matter of physical capacities? Physiol. Behav.

793   **151**: 448–455. doi:10.1016/j.physbeh.2015.08.001.

794 Pujolar, J.M., Bevacqua, D., Andrello, M., Capoccioni, F., Ciccotti, E., De Leo, G.A., and Zane, L. 2011.

795   Genetic patchiness in European eel adults evidenced by molecular genetics and population

796   dynamics   modelling.   Mol.   Phylogenet.   Evol.   **58**(2):   198–206.
797   doi:10.1016/j.ympev.2010.11.019.

798 Pujolar, J.M., Jacobsen, M.W., Als, T.D., Frydenberg, J., Munch, K., Jónsson, B., Jian, J.B., Cheng, L.,
799   Maes, G.E., Bernatchez, L., and Hansen, M.M. 2014. Genome-wide single-generation
800   signatures of local selection in the panmictic European eel. Mol. Ecol. **23**(10): 2514–2528.
801   doi:10.1111/mec.12753.

802 Railsback, S.F., and Harvey, B.C. 2013. Trait-mediated trophic interactions: is foraging theory keeping
803   up? Trends Ecol. Evol. **28**(2): 119–125. doi:10.1016/j.tree.2012.08.023.

804 Rougier, T., Lassalle, G., Drouineau, H., Dumoulin, N., Faure, T., Deffuant, G., Rochard, E., and
805   Lambert, P. 2015. The Combined Use of Correlative and Mechanistic Species Distribution
806   Models Benefits Low Conservation Status Species. PLOS ONE **10**(10): e0139194.
807   doi:10.1371/journal.pone.0139194.

808 Scheiner, S.M. 1993. Genetics and Evolution of Phenotypic Plasticity. Annu. Rev. Ecol. Syst. **24**: 35–68.

809 Schlichting, C.D. 1986. The Evolution of Phenotypic Plasticity in Plants. Annu. Rev. Ecol. Syst. **17**(1):
810   667–693. doi:10.1146/annurev.es.17.110186.003315.

811 Sultan, S.E. 1987. Evolutionary Implications of Phenotypic Plasticity in Plants. *In* Evolutionary Biology.
812   *Edited by* M.K. Hecht, B. Wallace, and G.T. Prance. Springer US. pp. 127–178.

813 Tesch, F.-W. 2003. The eel. *In* 3rd ed. Blackwell Science, Oxford, UK.

814 Travis, J. 1994. Evaluating the adaptive role of morphological plasticity. *In* Ecological Morphology.
815   *Edited by* P. Wainwright and S. Reilly. University of Chicago Press. pp. 99–122.

816 Ulrik, M.G., Pujolar, J.M., Ferchaud, A.-L., Jacobsen, M.W., Als, T.D., Gagnaire, P.A., Frydenberg, J.,
817   Bøcher, P.K., Jónsson, B., Bernatchez, L., and others. 2014. Do North Atlantic eels show
818   parallel patterns of spatially varying selection? BMC Evol. Biol. **14**(1): 138.

819 Varley, C.G., Gradwell, G.R., and Hassell, M.P. 1973. Insect population ecology an analytical approach.
820   University of California Press, California.

821 Vélez-Espino, L.A., and Koops, M.A. 2010. A synthesis of the ecological processes influencing variation
822   in life-history and movement patterns of American eel: towards a global assessment. Rev.
823   Fish Biol. Fish. **20**(2): 163–186. doi:10.1007/s11160-009-9127-0.

824 Vollestad, L.A. 1992. Geographic Variation in Age and Length at Metamorphosis of Maturing
825   European Eel: Ennvironmental Effects and Phenotypic Plasticity. J. Anim. Ecol. **61**(1): 41–48.

826 Weiner, J. 1990. Asymmertic Competition in Plant Population. Tree **5**(11): 360–364.

827 Williams, G.C. 1996. Adaptation and natural selection: a critique of some current evolutionary
828   thought. Princeton Univ. Press, Princeton, NJ.

829

830 **Tables**

831 **Table 1.** GenEveel parameter descriptions with reference values and modalities (- and +) for the 17

832 parameters involved in the experimental design.

Parameter	Description	Reference value	(-) modality	(+) modality	Reference
n	Cells of river catchment	30	24	36	(Drouineau et al. 2014)
N	Number of glass eels that colonize freshwater	30 000	24 000	36 000	(Drouineau et al. 2014)
$a1$	Regression coefficient from fecundity at length	8 846	-	-	(Andrello et al. 2011)
a	Regression coefficient from fecundity at length	1.3877119	-	-	(Melià et al. 2006, Andrello et al. 2011)
b	Regression exponent from fecundity at length	3.22	2.576	3.864	(Melià et al. 2006)
L_∞ (cm)	Asymptotic length	76.2	60.96	91.44	(De Leo and Gatto 1995)
L_{sm} (cm)	Male length at silvering	40.5	38.15	42.85	(Vollestad 1992)
L_g (cm)	Length at recruitment	7.5	6	9	(Desaunay and Guerault 1997, Dekker 1998, Desaunay et al. 2012)
$fertility$	Constant of male fertility	43	40.5	45.5	-
$K_{fast}(i,1)$, year^{-1}	Fast intrinsic growth rate	0.315	0.295	0.335	(De Leo and Gatto 1995)
$K_{slow}(i,1)$, year^{-1}	Slow intrinsic growth rate	0.253	0.233	0.273	(De Leo and Gatto 1995)
$propK$	Proportion of individuals that grow slowly	0.5	0.4	0.6	-
$M_{fast}(i,1)$, year^{-1}	Fast intrinsic mortality rate	0.38	0.405	0.355	-
$M_{slow}(i,1)$, year^{-1}	Slow intrinsic mortality rate	0.138	0.15	0.127	(Dekker 2000)
α	Intensity of density-dependence	0.0001	0.00008	0.00012	(Drouineau et al. 2014)
r_K	Ratio between upstream and downstream growth rate	0.5	0.4	0.6	(Drouineau et al. 2014)
r_M	Ratio between upstream and downstream mortality	1	0.8	1.02	(Drouineau et al. 2014)

	rate				
Y_K	Shape parameter of growth	0.05	0.049	0.051	(Drouineau et al. 2014)
Y_M	Shape parameter of mortality	0.05	0.049	0.051	(Drouineau et al. 2014)

833

35

834   **Table 2.** Results of Mann-Kendall test of reference simulation.

Spatial pattern	Tau
Abundance	-1
Mean length at silvering	0.98
Sex ratio (proportion of females)	0.57
Ratio of fast growers	-0.78
Mean realized growth rate	-1

835

836   **Table 3.** Number of simulations with consistent patterns for each modality of the groups of

837   parameters, over the number of simulations for which it was possible to calculate a pattern. The

838   columns represent the spatial patterns and the numbers of simulations for which it was possible to

839   estimate a pattern.

Parameters group	Abundance 2560	Mean length at silvering 1920	Sex ratio (proportion of females) 1610	Ratio of fast growers 2560	Mean realized growth rate 2560	The five spatial patterns 1610
N	(-) 1280/1280	(-) 650/960	(-) 70/800	(-) 1280/1280	(-) 1280/1280	(-) 70/800
	(+) 1280/1280	(+) 650/960	(+) 60/810	(+) 1280/1280	(+) 1280/1280	(+)60/810
fertility and L_{sm}	(-) 1280/1280	(-) 800/960	(-) 130/800	(-) 1280/1280	(-) 1280/1280	(-)130/800
	(+) 1280/1280	(+) 500/960	(+) 0/810	(+) 1280/1280	(+) 1280/1280	(+) 0/810
$K_{fast}(i, 1)$ and $M_{fast}(i, 1)$	(-) 1280/1280	(-) 650/960	(-) 70/810	(-) 1280/1280	(-) 1280/1280	(-) 70/810
	(+) 1280/1280	(+) 650/960	(+) 60/800	(+) 1280/1280	(+) 1280/1280	(+) 60/800
$K_{slow}(i, 1)$ and $M_{slow}(i, 1)$	(-) 1280/1280	(-) 710/960	(-) 0/810	(-) 1280/1280	(-) 1280/1280	(-) 0/810
	(+) 1280/1280	(+) 590/960	(+) 130/800	(+) 1280/1280	(+) 1280/1280	(+) 130/800
propK	(-) 1280/1280	(-) 650/960	(-) 90/810	(-) 1280/1280	(-) 1280/1280	(-) 90/810
	(+) 1280/1280	(+) 650/960	(+) 40/800	(+) 1280/1280	(+) 1280/1280	(+) 40/800
α	(-) 1280/1280	(-) 810/960	(-) 60/960	(-) 1280/1280	(-) 1280/1280	(-) 60/960
	(+) 1280/1280	(+) 490/960	(+) 70/650	(+) 1280/1280	(+) 1280/1280	(+) 70/650
n	(-) 1280/1280	(-) 660/960	(-) 60/810	(-) 1280/1280	(-) 1280/1280	(-) 60/810
	(+) 1280/1280	(+) 640/960	(+) 70/800	(+) 1280/1280	(+) 1280/1280	(+) 70/800
b	(-) 1280/1280	(-) 360/640	(-) 10/640	(-) 1280/1280	(-) 1280/1280	(-) 10/640
	(+) 1280/1280	(+) 940/1280	(+) 120/970	(+) 1280/1280	(+) 1280/1280	(+) 120/970
L_∞	(-) 1280/1280	(-) 310/640	(-) 120/640	(-) 1280/1280	(-) 1280/1280	(-) 120/640
	(+) 1280/1280	(+) 990/1280	(+) 10/970	(+) 1280/1280	(+) 1280/1280	(+) 10/970
L_g	(-) 1280/1280	(-) 650/960	(-) 60/800	(-) 1280/1280	(-) 1280/1280	(-) 60/800
	(+) 1280/1280	(+) 650/960	(+) 70/810	(+) 1280/1280	(+) 1280/1280	(+) 70/810
r_k and r_m	(-) 1280/1280	(-) 630/960	(-) 40/810	(-) 1280/1280	(-) 1280/1280	(-) 40/810
	(+) 1280/1280	(+) 670/960	(+) 90/800	(+) 1280/1280	(+) 1280/1280	(+) 90/800
γ_k and γ_m	(-) 1280/1280	(-) 730/960	(-) 60/810	(-) 1280/1280	(-) 1280/1280	(-) 60/810
	(+) 1280/1280	(+) 570/960	(+) 70/800	(+) 1280/1280	(+) 1280/1280	(+) 70/800

840   **Table 4.** Results of the 13 combinations that generated five consistent patterns. The signs +/- refer to

841   the modalities of the parameters groups. The two last columns represent the five spatial patterns. An

842   ascendant arrows stands for positive Mann-Kendall tau value (increasing trend from downstream to

843   upstream). Conversely, a descendant arrow stands for a negative Mann-Kendall tau value.

	N	fertility, L_{sm}	$K_{fast}(i, 1)$, $M_{fast}(i, 1)$	$K_{slow}(i, 1)$, $M_{slow}(i, 1)$	$propK$	α	n	b	L_∞	L_g	r_K, r_M	γ_K, γ_M	Abundance Ratio of fast growers $\overline{K(\iota,x)}$	Sex ratio $\overline{Ls}$
1	-	-	-	+	+	+	+	+	-	-	+	+	↘	↗
2	+	-	-	+	-	+	+	+	-	+	+	+	↘	↗
3	+	-	-	+	+	-	+	+	-	+	+	-	↘	↗
4	-	-	-	+	-	-	+	+	-	-	+	-	↘	↗
5	+	-	+	+	+	-	-	+	-	-	+	-	↘	↗
6	+	-	-	+	-	-	-	+	-	+	-	-	↘	↗
7	-	-	-	+	-	+	+	-	+	+	+	+	↘	↗
8	-	-	+	+	-	-	-	+	-	+	+	-	↘	↗
9	-	-	+	+	+	+	-	+	-	+	+	+	↘	↗
10	-	-	+	+	-	+	+	+	-	+	-	+	↘	↗
11	+	-	+	+	-	+	-	+	-	-	+	+	↘	↗
12	-	-	-	+	-	+	-	+	-	-	-	+	↘	↗
13	+	-	+	+	-	-	+	+	-	-	-	-	↘	↗

844

845 **Figures**

846

847 **Fig. 1.** Flow chart representing the fish biological pathway.

848
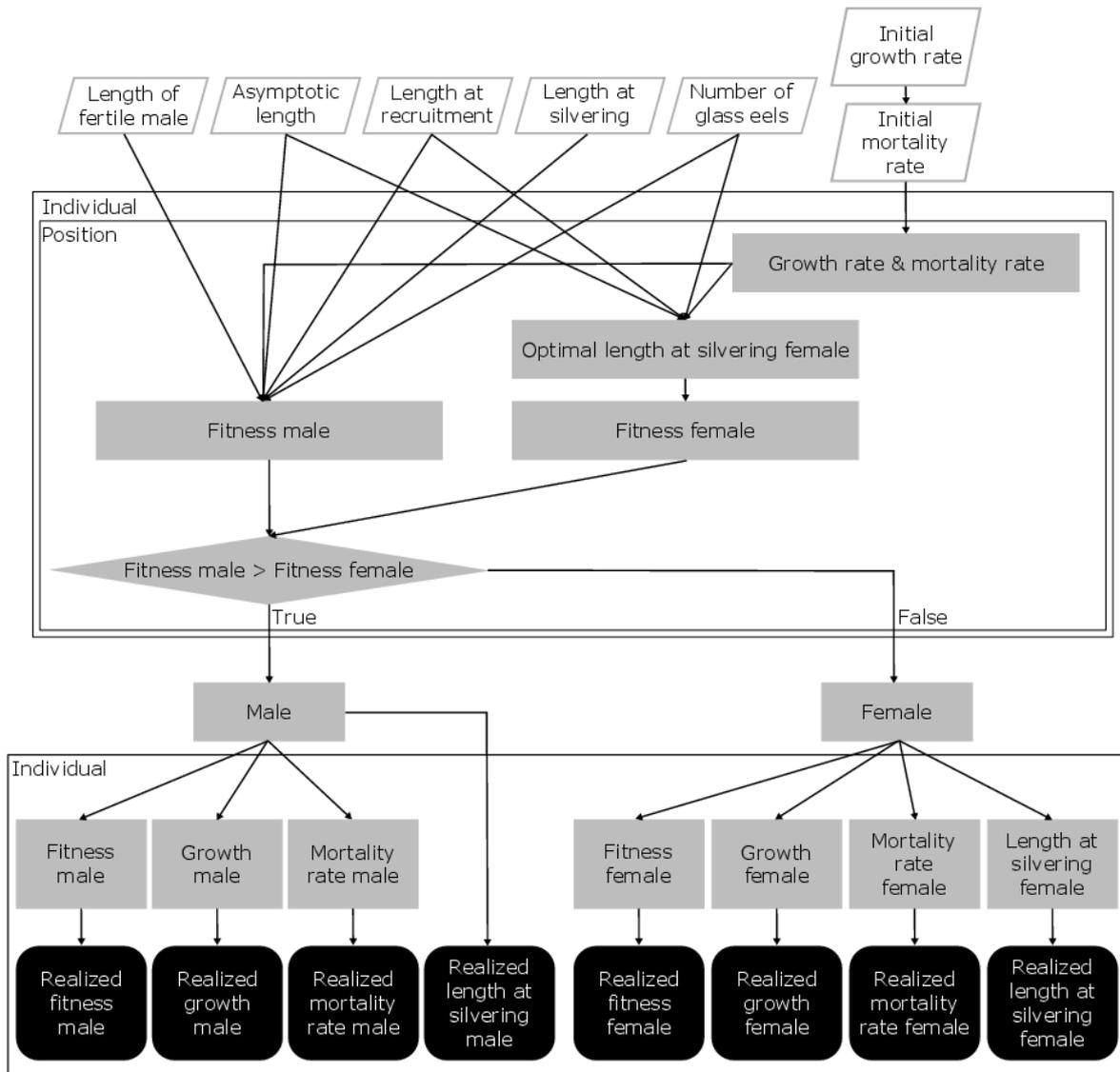
849

850 **Fig. 2.** Algorithm of the model GenEveel.

851

852
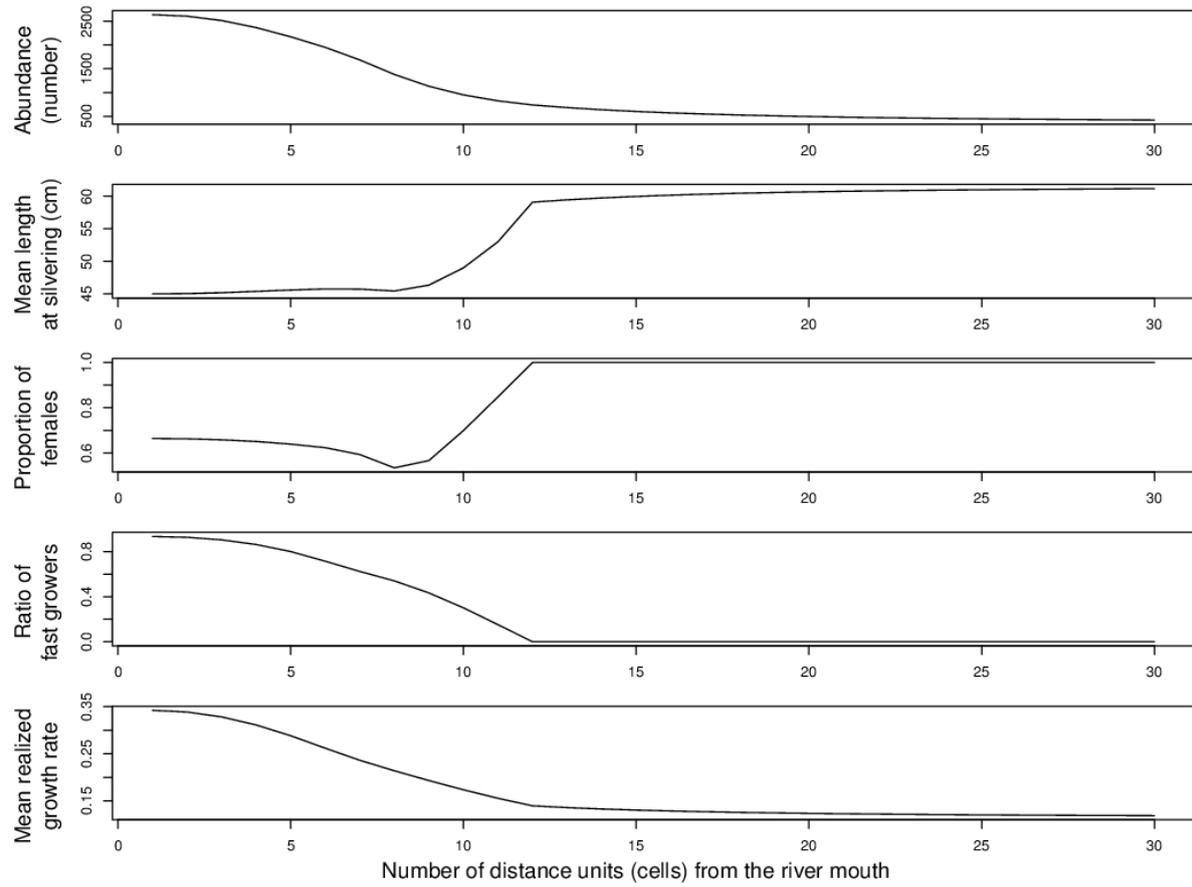
Fig. 3. Output values for the five spatial patterns resulting from the reference simulation.

854
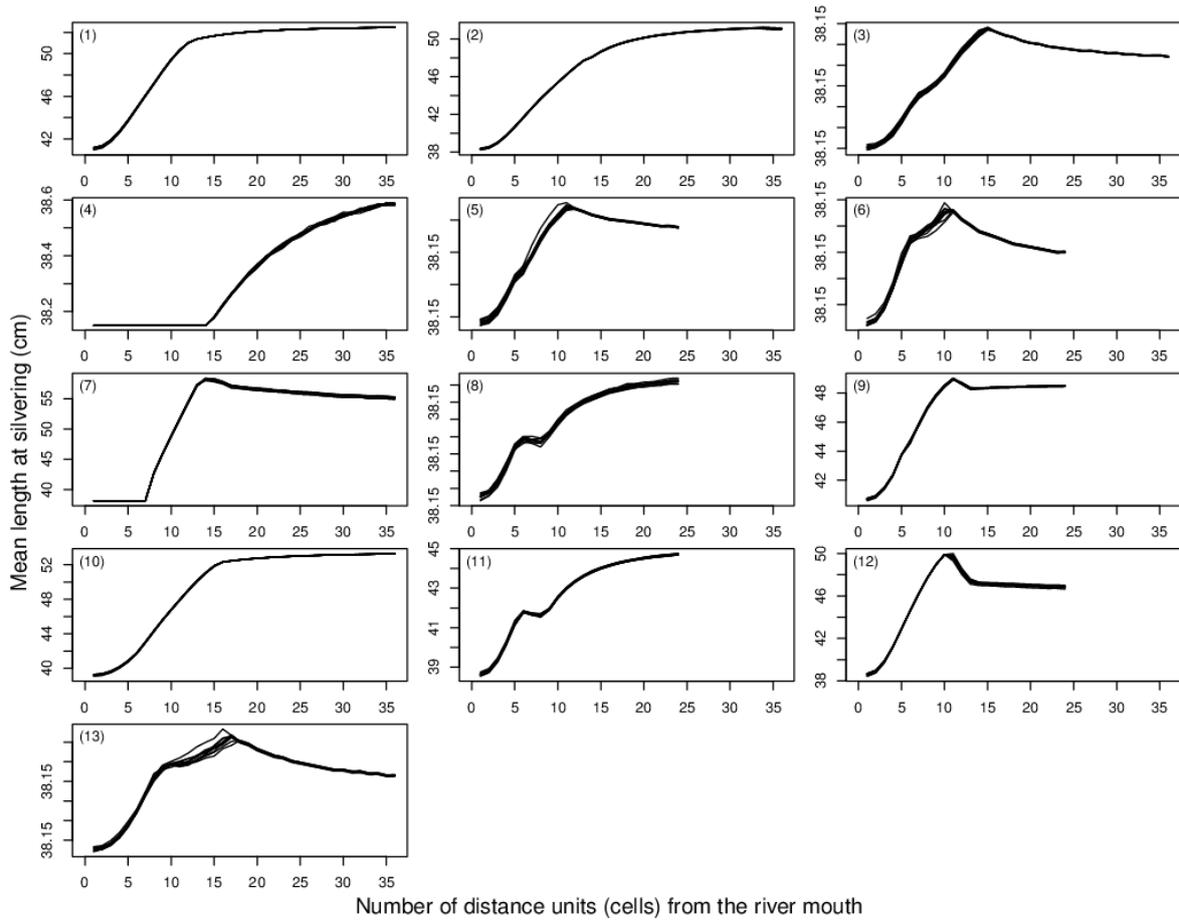
Fig. 4. Simulated mean length at silvering patterns in the 13 combinations of parameters that consistently mimic the pattern described in the literature. These 13 combinations correspond to the 13 combinations that generate consistent patterns for all the five spatial patterns. Each plot stands for a combination (the number is an identifier of the combination that can be found in table 4) and each line stands for a replicate.

862
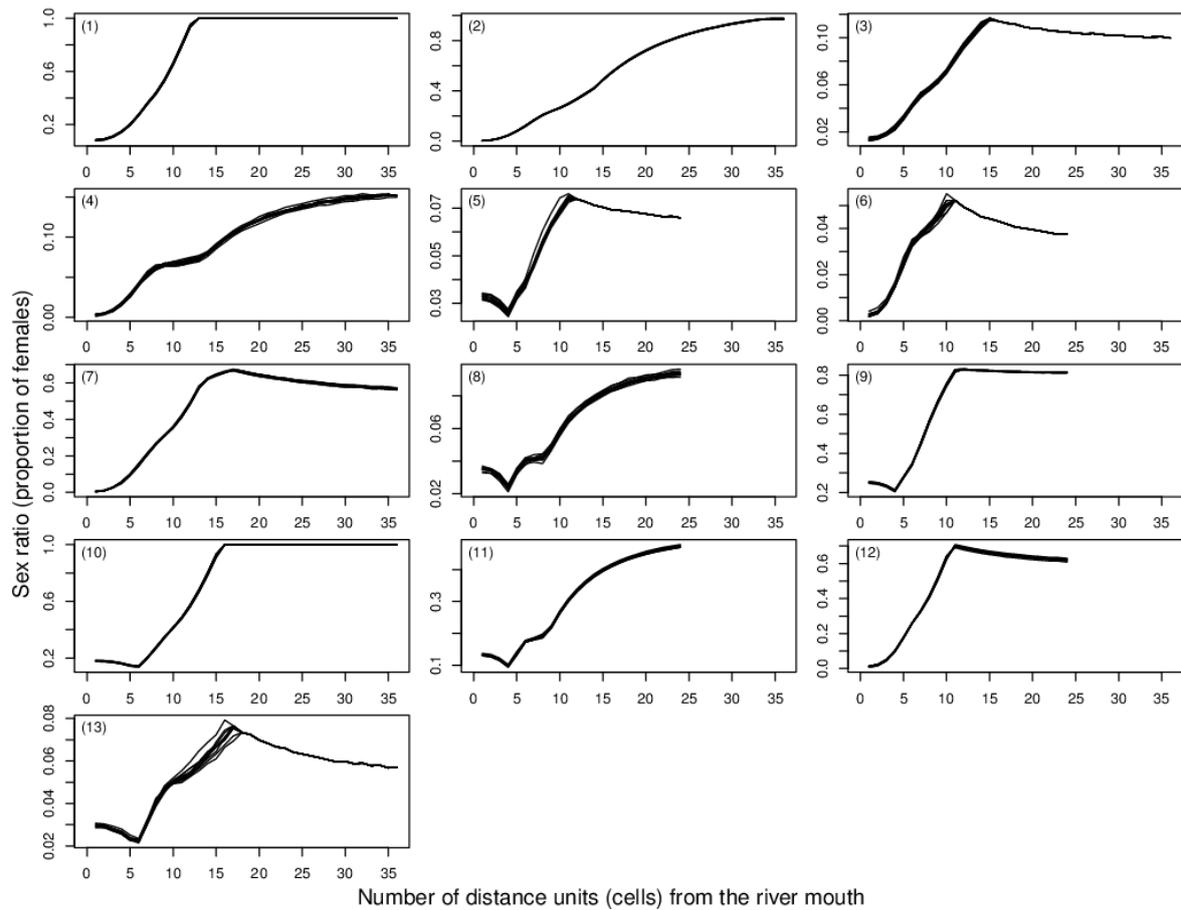
Fig. 5. Simulated sex ratio (proportions of females) patterns in the 13 combinations of parameters

that consistently mimic the pattern described in the literature. These 13 combinations correspond to

the 13 combinations that generate consistent patterns for all the five spatial patterns. Each plot

stands for a combination (the number is an identifier of the combination that can be found in table

4) and each line stands for a replicate.

868   **Supplemental Information**

869   **Table S1.** Results of the 256 combinations. The signs +/- refer to the modalities of the parameters

870   groups . The last five columns represent the spatial patterns. An ascendant arrows stands for positive

871   Mann-Kendall tau value (increasing trend from downstream to upstream). Conversely, a descendant

872   arrow stands for a negative Mann-Kendall tau value.